Angewandte
Communications

Electrochemical Polymerization

DOI: 10.1002/anie.201410598

Simplified Electrochemically Mediated Atom Transfer Radical Polymerization using a Sacrificial Anode[**]

*Sangwoo Park, Paweł Chmielarz, Armando Gennaro, and Krzysztof Matyjaszewski**

Abstract: *Simplification of electrochemically mediated atom transfer radical polymerization was achieved efficiently under either potentiostatic or galvanostatic conditions using an aluminum wire sacrificial anode (seATRP) immersed directly into the reaction flask without separating the counter electrode. seATRP polymerizations were carried out under different applied potentials,* E_{app}*s* $= E_{1/2}$, E_{pc}, E_{pc} -40 *mV, and* E_{pc} -80 *mV. As the rate of polymerization (*R_p*) can be modulated by applying different* E_{app} *potentials, more reducing conditions resulted in faster* R_p*. The polymerization results showed similar narrow molecular-weight distribution throughout the reactions, similar to results observed for n-butyl acrylate (BA) polymerization under conventional eATRP. High-molecular-weight PBA and diblock copolymers were synthesized by seATRP with more than 90 % monomer conversion. Furthermore, galvanostatic conditions were developed for synthesizing PBA with the two-electrode system.*

There has been interest recently in controlling polymerization by external stimuli, such as chemical, microwave, light, or electrical current.[1] Reactions can be potentially stopped and restarted by changing the stimulus.[1c,2] The recently developed electrochemically mediated atom transfer radical polymerization (*e*ATRP) is an example of such a procedure and has been used for the preparation of polymers with predetermined molecular weight and uniform structure under potentiostatic or galvanostatic conditions.[1e,3] In an *e*ATRP, activators, typically a copper(I)/ligand (Cu^I/L) complex, can be generated near the working electrode surfaces by the reduction of oxidatively stable deactivators ($Cu^{II}X/L$) under applied potential (E_{app}). The activator (Cu^I/L) is then homogeneously distributed throughout the reaction mixture by vigorous stirring and reaction of the activator with initiators (for example, alkyl halide, R−X) forms the radical species ($R^•$) and the oxidized catalyst ($Cu^{II}X/L$).[3a] Subsequently, the radical species propagate to form polymeric chains by reacting with monomers (M) or are reverted back to the dormant species (P_n−X) by reaction with the formed $Cu^{II}X/L$ deactivator complex. By repeating such sequential reactions, well-defined polymers can be obtained with uniform structures (Scheme 1).

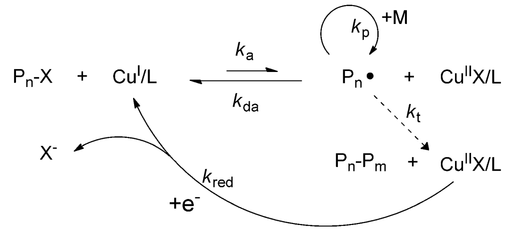

Scheme 1. Mechanism of *e*ATRP.

*e*ATRP can be carried out with low levels of catalysts, down to ppm of monomer concentration, and can be stopped and restarted by switching the applied potential, and *e*ATRP has been successfully used for the synthesis of materials with well-defined polymeric architectures.[3a,4] However, there are some limitations associated with *e*ATRP, especially in the reaction setup stage. Typically, *e*ATRP polymerizations can be achieved by utilizing a three-electrode system, allowing application of a potentiostatic process, that is, at constant applied potential. This requires the presence of a working electrode (WE), a counter electrode (CE), and a reference electrode (RE). In general, a platinum mesh electrode is selected as a WE, which provides a high surface area for effectively converting Cu^{II} into Cu^I. The RE is separated from the reaction solution by a supporting electrolyte saturated methylated cellulose (Tylose) gel, such as Ag/AgI/I^-, and the applied potential is determined by the WE and RE. The CE is generally a Pt mesh electrode that is also separated from the reaction mixture, in a similar manner to the RE, to avoid undesired side reactions, for example oxidation of Cu^I and contamination of the working solution by oxidation products.[1e] When an *e*ATRP was attempted with a directly immersed CE (Pt mesh), the results showed no polymerization (Figure 1, triangles). This could be due to Cu^I/L oxidation, leading to the formation of a bare Cu^{II} deactivator. Therefore, separation of the CE from the polymerization mixture is necessary in a conventional *e*ATRP. Herein, a significant simplification of the procedures used for an *e*ATRP is reported by using a sacrificial counter electrode, (*se*ATRP) which does not require any separation and can be

---

[*] S. Park, P. Chmielarz, K. Matyjaszewski
Department of Chemistry, Carnegie Mellon University
4400 Fifth Avenue, Pittsburgh, PA 15213 (USA)
E-mail: km3b@andrew.cmu.edu

P. Chmielarz
Department of Physical Chemistry, Faculty of Chemistry
Rzeszow University of Technology
Al. Powstańców Warszawy 6, 35-959 Rzeszow (Poland)

A. Gennaro
Dipartimento di Scienze Chimiche, Università di Padova
via Marzolo 1, 35131 Padova (Italy)

[**] The funding support from NSF (CHE 1400052) is gratefully appreciated.

Supporting information for this article is available on the WWW under http://dx.doi.org/10.1002/anie.201410598.

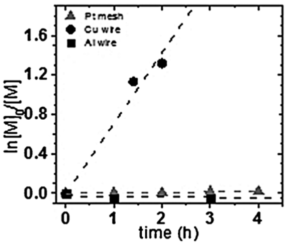

Figure 1. ATRP with 10 cm metal wires ($d = 1$ mm). Pt mesh = *e*ATRP carried out with a Pt mesh cathode and a directly immersed Pt mesh counter electrode.

directly inserted into the reaction mixture. There are two potential advantages of using *se*ATRP. The first is the use of an undivided cell, which allows for a simpler, lower-cost process, and most of all, the minimization of the ohmic drop, bringing a beneficial energy saving. The second advantage is the possibility of a galvanostatic process using two electrode system and a current generator, which is simpler than a potentiostat. Both advantages should benefit commercial and academic efforts in the area of *e*ATRP.

In the ideal case of *se*ATRP, the sacrificial counter electrode should not react with the Cu/L catalysts either in the presence or absence of an applied electric current. Instead, the electrode can only be self-consumed ($M_t \rightarrow M_t^{n} + n e^-$) under an applied current, which also prevents undesired side reactions, in particular formation of bare deactivators. Copper and aluminum metal wires ($l = 10$ cm and $d = 1$ mm) were prepared and, first of all, tested for their inertness under polymerization conditions, that is, by immersing in the solution mixed with monomer, initiator, and $CuBr_2$/TPMA. The Cu wire acted as both a supplemental activator and a reducing agent (SARA),[1g,4g,5] the reaction showed more than 74% monomer conversion in 2 h. On the other hand, Al wire showed no reduction of Cu^{II}/L to Cu^{I}/L even though Al has a negative standard potential ($E^0 = -1.66$ V vs. SHE in water). This is likely because the surface of the Al wire is passivated by forming stable oxidized layers to prevent reduction of Cu^{II}/L to Cu^{I}/L. Therefore the Al wire seemed to fit the requirements of a sacrificial electrode.

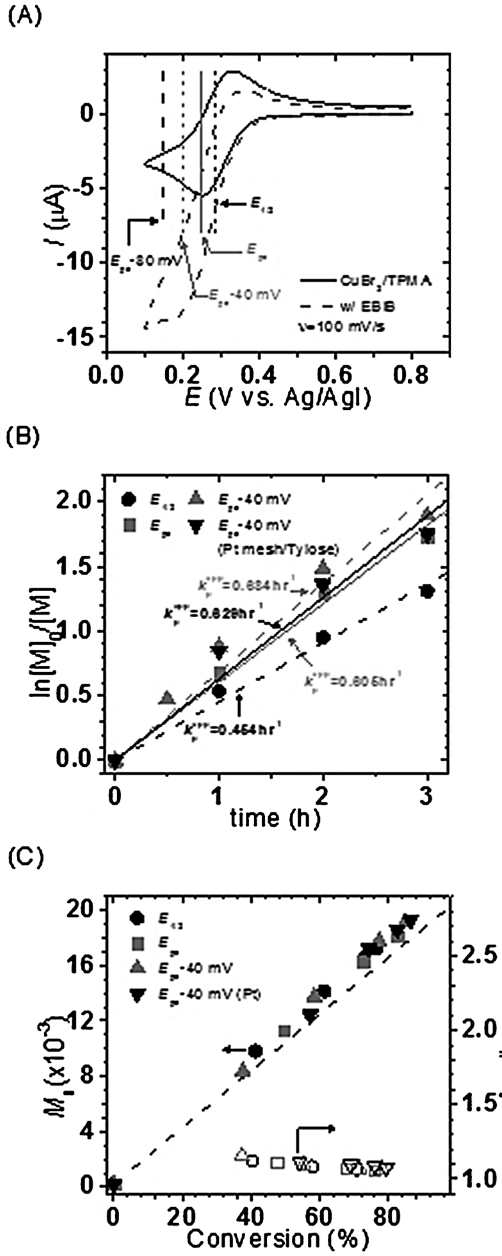

Figure 2. A) Cyclic voltammetry of $CuBr_2$/TPMA with and without initiator (lines indicate E_{app}); B) First-order kinetic plot with different E_{app} values; and C) M_n and M_w/M_n versus conversion of BA polymerizations by *se*ATRP.

A series of *n*-butyl acrylate (BA) polymerizations was carried out under potentiostatic conditions with a Pt mesh WE, an Al CE, and Ag/AgI/I^- RE. Control over the rate of polymerization (R_p) was evaluated by applying different constant potentials E_{app}. Four E_{app} values were selected: $E_{1/2}$, E_{pc}, E_{pc}−40 mV, and E_{pc}−80 mV (Figure 2A). Faster R_p was observed when more negative potentials were applied. The fastest apparent propagation rate constant (k_p^{app}) was observed to be 0.684 h^{-1} ($E_{app} = E_{pc}$−40 mV). This value was 1.5 times faster than when $E_{app} = E_{1/2}$. The k_p^{app} values of *se*ATRP and conventional *e*ATRP with $E_{app} = E_{pc}$−40 mV are well-matched (Table 1, entries 3 and 4) and identical cathodic current drops were observed (Supporting Information, Figure S1). All of the BA polymerizations by *se*ATRP showed good evolution of molecular weight (MW), close to theoretical values, and maintained narrow molecular-weight distributions (M_w/M_n). After the polymerization was completed, a scanning electron microscope (SEM) was used for the examination of the surfaces of the Al wires. Pristine Al wires showed clear surfaces; however, the surfaces of Al wires showed porous morphologies after the application of current during a *se*ATRP (Supporting Information, Figure S2). The pores on the surface of the wires could be formed by oxidation of aluminum (to Al^{3+}) and reaction with residual water molecules to form Al_2O_3.[6] The overall weight loss of the wire was less than 1 mg (Supporting Information, Table S1), in agreement with chronoamperometry (Supporting Information, Table S1 and Figure S1). According to ICP-MS analysis, the residual amount of Al and Cu in isolated polymers was 5.2 and 16 ppm, respectively. These values are smaller than the

Table 1: Summary of *se*ATRP of BA.[a]

Entry	[M]/[I]/ [CuBr$_2$/TPMA]	E_{app}[b]	Conv. [%][c]	$M_{n,GPC}$ [g mol^{-1}][d]	$M_{n\ theoretical}$ [g mol^{-1}]	M_w/M_n[d]	k_p^{app} [h^{-1}]
1	160/1/0.02	$E_{1/2}$	76	17250	15800	1.06	0.454
2	160/1/0.02	E_{pc}	82	18150	17000	1.06	0.605
3	160/1/0.02	E_{pc}−40 mV	85	19100	17600	1.07	0.684
4[e]	160/1/0.02	E_{pc}−40 mV	86	19300	17800	1.08	0.629
5	1000/1/0.1	E_{pc}−80 mV	92	96700	118100	1.17	0.352
6	100/1/0.005	E_{pc}−80 mV	23	3400	3100	1.36	0.511
7	400/1/0.04	E_{pc}−80 mV	72	34800	40500	1.29	0.674
8	200/1/0.02	E_{pc}−80 mV	77	19200	19900	1.07	0.795
9	200/1/0.02	galvanostatic conditions[f]	78	18560	20100	1.07	0.788

[a] Polymerization conditions: WE = Pt mesh, CE = Al wire (l = 10 cm, d = 1 mm), RE = Ag/AgI/I$^-$, supporting electrolyte: tetrabutylammonium perchlorate (TBAP, 0.2 M), T = 50 °C. [b] E_{app} values were selected based on CV analysis without initiator (scan rate ν = 100 mV s^{-1}). [c] Final conversion, determined by ^{1}H NMR spectroscopy. [d] MW and MW distributions were determined by THF GPC with PMMA standards. [e] Using conventional *e*ATRP, CE = Pt mesh (separated from reaction mixture by supporting electrolyte saturated Tylose gel). [f] I_{app} = −1.03, −0.53, −0.40, and −0.28 mA for 30 min each step.

initial amount of oxidized aluminum and Cu, indicating partial removal of residual metals during polymer purification (see the Supporting Information).

The level of preservation of chain-end functionality was investigated by synthesis of high-molecular-weight PBA and by chain-extension experiments. Synthesis of high MW of PBA was examined by targeting a DP of 1000 (that is, [M]/[I] = 1000; Figure 3). A linear first-order kinetic plot was observed during the polymerization and the MWs of PBA matched well with the theoretical values below 60 % monomer conversion. Above 60 % monomer conversion the observed MWs showed a slight decrease from the theoretical values, presumably resulting either from transfer reactions or termination reactions (coupling and disproportionation). Although the MW values were slightly different from the ideal values, the final monomer conversion reached 90 % after 10 h and MW distributions were lower than 1.2. Chain end functionality was also evaluated by chain extension of a macroinitiator formed by *se*ATRP to form a block copolymer. A PBA with low DP was prepared by *se*ATRP (M_n = 3430 and M_w/M_n = 1.36; Supporting Information, Figure S3). The PBA$_{27}$−Br macroinitiator was then used in a chain extension copolymerization with *tert*-butyl acrylate (*t*BA) as the second monomer. Linear first-order kinetics was observed (Figure 4A), and GPC traces indicated good incorporation of the second monomer, as essentially a clean peak shift was observed (Figure 4C).

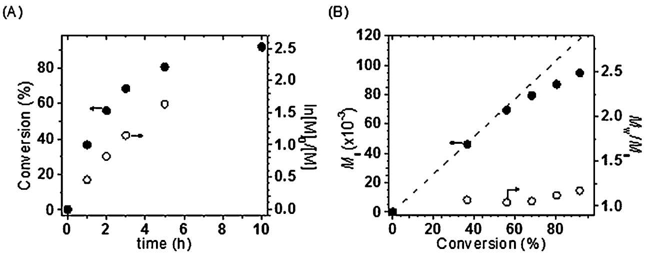

Figure 3. High MW of PBA by *se*ATRP. A) Conversion of monomers versus reaction time and B) MW evolution and MW distribution results by GPC with PMMA standards.

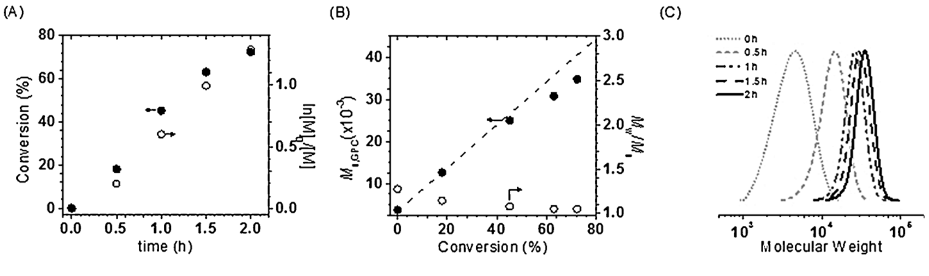

Figure 4. Chain extension by *se*ATRP. A) Conversion of monomers versus reaction time and B) MW evolution and MW distribution results from GPC with PMMA standards; C) GPC results of block copolymerization.

Polymerization under galvanostatic conditions (constant applied current) was carried out for the purpose of further simplifying the reaction setup, since galvanostatic conditions only require two electrodes: a Pt mesh working cathode and an Al wire counter/sacrificial anode (Supporting Information, Scheme S1). The applied currents I_{app} were determined by the polymerizations carried out under potentiostatic conditions. In general, two characteristic cathodic current responses are observed during the polymerization under potentiostatic conditions: an initial fast current decay followed by a nearly constant current (Figure 5A). The first response is mainly attributed to the reduction of initially used Cu^{II}X/L to Cu^{I}/L and reaction of R−X to form the propagating radical R$^\cdot$ and Cu^{II}X/L. Once the equilibrium is established between R−X, Cu^{I}/L, R$^\bullet$, and Cu^{II}X/L, an essentially constant current flow was observed owing to the maintenance of a constant concentration of Cu^{I}/L. On the basis of the chronoamperometry (CA) results, the total passed charge was calculated by integration of the CA area, that is, $Q(C) = A\,s$. Thus, two constant I_{app} values were used for the polymerization under galvanostatic conditions; $I_{app,1}$ = (−) 0.713 mA (for 0 to 1.2 h) and $I_{app,2}$ = (−) 0.297 mA (for 1.2 to 4 h), where negative values indicate cathodic current. The R_p showed a slight decrease from values observed under potentiostatic conditions when the second current was constantly applied ($I_{app,2}$; Supporting Information, Figure S4). The values observed for *se*ATRP under galvanostatic conditions

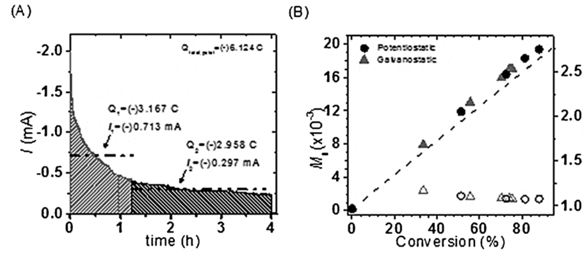

Figure 5. Galvanostatic *se*ATRP. A) chronoamperometry results from potentiostatic condition (exponentially drop) and applied current (dot line) and B) MW and MW distribution results from GPC with PMMA standards.

showed similar MW evolution and MW distribution values as compared to polymerizations conducted under potentiostatic conditions. Slow copper deposition on the WE surfaces was observed when applying $I_{\mathrm{app},2}$ (−0.297 mA). The Cu deposition arises from further reduction of $\mathrm{Cu^I/L}$ to $\mathrm{Cu^0}$, since under galvanostatic conditions the applied potentials cannot be exactly controlled. After the polymerization, the residual concentration of $\mathrm{Cu^{II}/L}$ in the solution reached 0.1 mM ($\lambda_{\mathrm{max,Cu^{II}/TPMA}} = 975$ nm, 20 ppm to monomer molar concentration), that is, overall 80 % of $\mathrm{Cu^{II}}$ had been removed from the reaction medium (Supporting Information, Figure S4). To improve controllability, and avoid undesirable Cu deposition, a multi-step current procedure was developed and applied to the reaction mixture. The applied currents were determined from potentiostatic conditions: −1.03, −0.53, −0.40, and −0.28 mA for $I_{\mathrm{app},1}$ to $I_{\mathrm{app},4}$, respectively (30 min for each step). Identical first-order kinetic plots were observed, and GPC analysis indicated similar MW evolution and a narrow MW distribution (Figure 6). As expected copper deposition on the WE surfaces was not observed in this case.

In conclusion, a simplified electrochemically mediated atom transfer radical polymerization was achieved by using a sacrificial counter electrode (*se*ATRP). The direct immersion of an Al wire counter electrode in the reaction medium can avoid additional preparation setup steps, and the polymerization results indicated good control of reaction kinetics, providing polymers with molecular weight evolution close to theoretical values and generating polymers with narrow molecular-weight distribution. The rate of the polymerizations R_p was controlled by applying different potentials E_{app}, with faster R_p observed using more negative E_{app}. Synthesis of high MW polymers and chain extension reactions indicate good conservation of chain-end functionalities. The *se*ATRP procedure can be further simplified by using only two electrodes and applying a constant current under galvanostatic conditions. The use of a multi-step current procedure showed identical results to polymerizations carried out under potentiostatic conditions, namely linear first-order kinetics and a uniform growth of polymers.

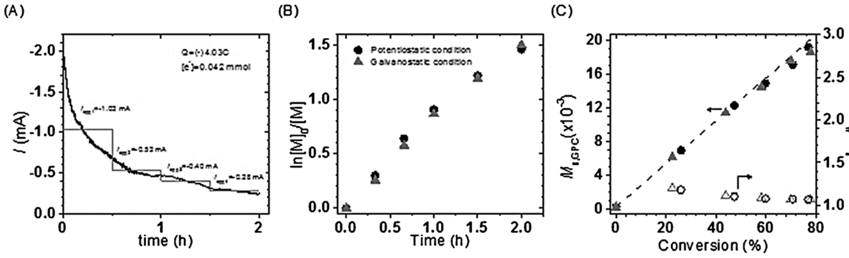

Figure 6. Multi-step chronoamperometry for galvanostatic *se*ATRP. A) chronoamperometry results from potentiostatic conditions (exponential drop) and applied current (dotted line), B) first-order kinetic plots by potentiostatic and galvanostatic conditions, and C) MW and MW distribution results from GPC with PMMA standards.

Received: October 30, 2014
Revised: November 30, 2014

Keywords: atom transfer radical polymerization · block copolymers · electrochemistry · sacrificial electrodes

[1] a) Z. P. Cheng, X. L. Zhu, M. Chen, J. Y. Chen, L. F. Zhang, *Polymer* **2003**, *44*, 2243; b) C. K. A. Gregson, V. C. Gibson, N. J. Long, E. L. Marshall, P. J. Oxford, A. J. P. White, *J. Am. Chem. Soc.* **2006**, *128*, 7410; c) S. Yamago, Y. Ukai, A. Matsumoto, Y. Nakamura, *J. Am. Chem. Soc.* **2009**, *131*, 2100; d) Y. Kwak, K. Matyjaszewski, *Macromolecules* **2010**, *43*, 5180; e) A. J. D. Magenau, N. C. Strandwitz, A. Gennaro, K. Matyjaszewski, *Science* **2011**, *332*, 81; f) F. A. Leibfarth, K. M. Mattson, B. P. Fors, H. A. Collins, C. J. Hawker, *Angew. Chem. Int. Ed.* **2013**, *52*, 199; *Angew. Chem.* **2013**, *125*, 210; g) D. Konkolewicz, Y. Wang, P. Krys, M. Zhong, A. A. Isse, A. Gennaro, K. Matyjaszewski, *Polym. Chem.* **2014**, *5*, 4396; h) T. G. Ribelli, D. Konkolewicz, S. Bernhard, K. Matyjaszewski, *J. Am. Chem. Soc.* **2014**, *136*, 13303; i) A. Anastasaki, V. Nikolaou, G. S. Pappas, Q. Zhang, C. Wan, P. Wilson, T. P. Davis, M. R. Whittaker, D. M. Haddleton, *Chem. Sci.* **2014**, *5*, 3536.

[2] a) B. P. Fors, C. J. Hawker, *Angew. Chem. Int. Ed.* **2012**, *51*, 8850; *Angew. Chem.* **2012**, *124*, 8980; b) S. Yamago, Y. Nakamura, *Polymer* **2013**, *54*, 981.

[3] a) A. J. D. Magenau, N. Bortolamei, E. Frick, S. Park, A. Gennaro, K. Matyjaszewski, *Macromolecules* **2013**, *46*, 4346; b) K. Matyjaszewski, *Macromolecules* **2012**, *45*, 4015.

[4] a) N. Bortolamei, A. A. Isse, A. J. D. Magenau, A. Gennaro, K. Matyjaszewski, *Angew. Chem. Int. Ed.* **2011**, *50*, 11391; *Angew. Chem.* **2011**, *123*, 11593; b) B. Li, B. Yu, W. T. S. Huck, F. Zhou, W. Liu, *Angew. Chem. Int. Ed.* **2012**, *51*, 5092; *Angew. Chem.* **2012**, *124*, 5182; c) S. Park, H. Y. Cho, K. B. Wegner, J. Burdynska, A. J. D. Magenau, H.-j. Paik, S. Jurga, K. Matyjaszewski, *Macromolecules* **2013**, *46*, 5856; d) B. Li, B. Yu, W. T. S. Huck, W. Liu, F. Zhou, *J. Am. Chem. Soc.* **2013**, *135*, 1708; e) S. S. Hosseiny, P. van Rijn, *Polymers* **2013**, *5*, 1229; f) B. Li, B. Yu, F. Zhou, *Macromol. Rapid Commun.* **2013**, *34*, 246; g) K. Matyjaszewski, N. V. Tsarevsky, *J. Am. Chem. Soc.* **2014**, *136*, 6513; h) F. Plamper, *Colloid Polym. Sci.* **2014**, *292*, 777.

[5] a) K. Matyjaszewski, N. V. Tsarevsky, W. A. Braunecker, H. Dong, J. Huang, W. Jakubowski, Y. Kwak, R. Nicolay, W. Tang, J. A. Yoon, *Macromolecules* **2007**, *40*, 7795; b) Y. Zhang, Y. Wang, K. Matyjaszewski, *Macromolecules* **2011**, *44*, 683; c) D. Konkolewicz, Y. Wang, M. Zhong, P. Krys, A. A. Isse, A. Gennaro, K. Matyjaszewski, *Macromolecules* **2013**, *46*, 8749; d) M. Zhong, Y. Wang, P. Krys, D. Konkolewicz, K. Matyjaszewski, *Macromolecules* **2013**, *46*, 3816; e) C.-H. Peng, M. Zhong, Y. Wang, Y. Kwak, Y.

Zhang, W. Zhu, M. Tonge, J. Buback, S. Park, P. Krys, D. Konkolewicz, A. Gennaro, K. Matyjaszewski, *Macromolecules* **2013**, *46*, 3803; f) Y. Wang, M. Zhong, W. Zhu, C.-H. Peng, Y. Zhang, D. Konkolewicz, N. Bortolamei, A. A. Isse, A. Gennaro, K. Matyjaszewski, *Macromolecules* **2013**, *46*, 3793; g) D. Konkolewicz, P. Krys, J. R. Gois, P. V. Mendonca, M. Zhong, Y. Wang, A. Gennaro, A. A. Isse, M. Fantin, K. Matyjaszewski, *Macromolecules* **2014**, *47*, 560; h) P. V. Mendonca, D. Konkolewicz, S. E. Averick, A. C. Serra, A. V. Popov, T. Guliashvili, K. Matyjaszewski, J. F. J. Coelho, *Polym. Chem.* **2014**, *5*, 5829.

[6] a) G. E. Thompson, *Thin Solid Films* **1997**, *297*, 192; b) Z. Su, G. Hahner, W. Zhou, *J. Mater. Chem.* **2008**, *18*, 5787.